Adiabatic and non-adiabatic cluster collisions(*)

R. SCHMIDT(1), O. KNOSPE(1) and U. SAALMANN(2)

(1) *Institut für Theoretische Physik, TU Dresden, 01062 Dresden, Germany*
(2) *Max-Planck-Institut für Physik komplexer Systeme*
Nöthnitzer Str. 38 - 01187 Dresden Germany

(ricevuto il 29 Settembre 1997; approvato il 15 Ottobre 1997)

Summary. — Adiabatic collisions (fusion, deep inelastic scattering) between two fullerenes are investigated on the basis of *Quantum Molecular Dynamics*. As a first application of the so-called *Non-adiabatic Quantum Molecular Dynamics*, developed recently, the non-adiabatic mechanism of collision induced dissociation in metallic clusterion–atom collisions is studied.

PACS 34.10 – General theories and models of atomic and molecular collisions and interactions (including statistical theories, transition state, stochastic and trajectory models, etc.).
PACS 34.50 – Scattering of atoms, molecules, and ions.
PACS 36.40 – Atomic and molecular clusters.
PACS 01.30.Cc – Conference proceedings.

1. – Introduction

The field of cluster collisions represents an exciting new branch of collision physics. It is particularly a challenging field due to the large but finite numbers of electronic *and* atomic degrees of freedom invoked. According to these degrees of freedom one can distinguish two basically different types of collisions:

i) *adiabatic collisions*, where electronic transitions do not occur or at least they are unimportant in order to understand the reaction mechanism, and

ii) *non-adiabatic collisions*, where electronic excitation, ionization and charge transfer appear and/or the phenomena related to these transitions are just the quantities of interest.

(*) Paper presented at the 174. WE-Heraeus-Seminar "New Ideas on Clustering in Nuclear and Atomic Physics", Rauischholzhausen (Germany), 9-13 June 1997.

Adiabatic cluster collisions show remarkable analogies in their mechanisms to that known in nuclear heavy-ion reactions [1, 6]. Non-adiabatic cluster collisions build the bridge between ion-atom scattering and ion-surface interaction.

Microscopically, adiabatic cluster collisions can be studied by quantum molecular dynamics (QMD). In QMD, classical atomic motion is treated simultaneously and self-consistently with a quantum–mechanical description of the electronic structure of the ground state. In practical realizations of QMD, different approximations have been applied to solve the electronic problem: density functional theory (DFT) in local density approximation (LDA) [7, 8], approximate LDA [9], Hartree-Fock theory [10], and the tight binding method [11]. As a typical example of adiabatic processes, (deep) inelastic scattering and fusion between two fullerenes are investigated in sect. **2**, using QMD. The results are compared with recent experiments.

In contrast to adiabatic collisions, the self-consistent treatment of electronic *and* atomic degrees of freedom in non-adiabatic cluster collisions is still a challenging problem. Recently, the basic formalism of a so-called non-adiabatic quantum molecular dynamics (NA-QMD) has been developed [12], based on time-dependent density functional theory [13,14]. This universal approach treats simultaneously and self-consistently classical atomic motion and quantum electronic transitions in atomic many-body systems. As a first application of this theory, the mechanism of collision induced dissociation in metallic clusterion-atom collisions is studied in sect. **3** and the results are confronted with data of kinematic complete coincidence experiments.

2. – Collisions between fullerenes

Our systematic investigation of fullerene-fullerene collisions using QMD simulations includes at present $C_{60}^+ + C_{60}$ [5, 6], $C_{70}^+ + C_{60}$ and $C_{70}^+ + C_{70}$ collisions [4]. In this section, the fusion-relevant range of collision energies $50 < E_{\mathrm{cm}} < 250$ eV (in the center-of-mass frame) is considered. A large number of collision events was simulated for zero cluster temperature as well as for a temperature of $T = 2000$ K in both clusters.

The discriminating mechanism between fusion and scattering in these collisions can be recognized by investigating the kinetic energy as a function of time [5], which is shown for two $C_{60}^+ + C_{60}$ events in fig. 1. The general increase of the kinetic energy after the system has reached the distance of closest approach indicates that a part of the stored potential energy can be converted back into kinetic energy of relative motion. If this "bouncing-off" is suppressed (upper left part of fig. 1) due to the rearrangement of atoms in the contact zone, a fusion event will be detected, whereas if the increase of kinetic energy proceeds to a large enough extent (lower left part of fig. 1) the effective repulsion of the (more or less) intact fullerene structure leads to a scattering event [4].

In fusion events, strongly deformed (and highly excited) compound clusters are formed which resemble a "peanut"-like structure (see upper right part of fig. 1). The "memory" on the entrance channel (*i.e.* on the orientation) is lost in most cases. The large excitation energy in these compounds can be reduced by successive dimer evaporation [5, 15]. However, even *complete* fusion, *i.e.* C_{120}, C_{130}, and C_{140}, respectively, is observed experimentally [5, 15]. The stabilization of the fused compound against evaporation is a direct consequence of the formation of such "peanut" isomers, which drastically reduces the final vibrational energy [5].

The fusion barriers for the three considered systems at zero cluster temperature have been determined by varying the collision energy and (for each energy) the random rotation of both fullerenes. The values obtained are compared with the experimental data [15]

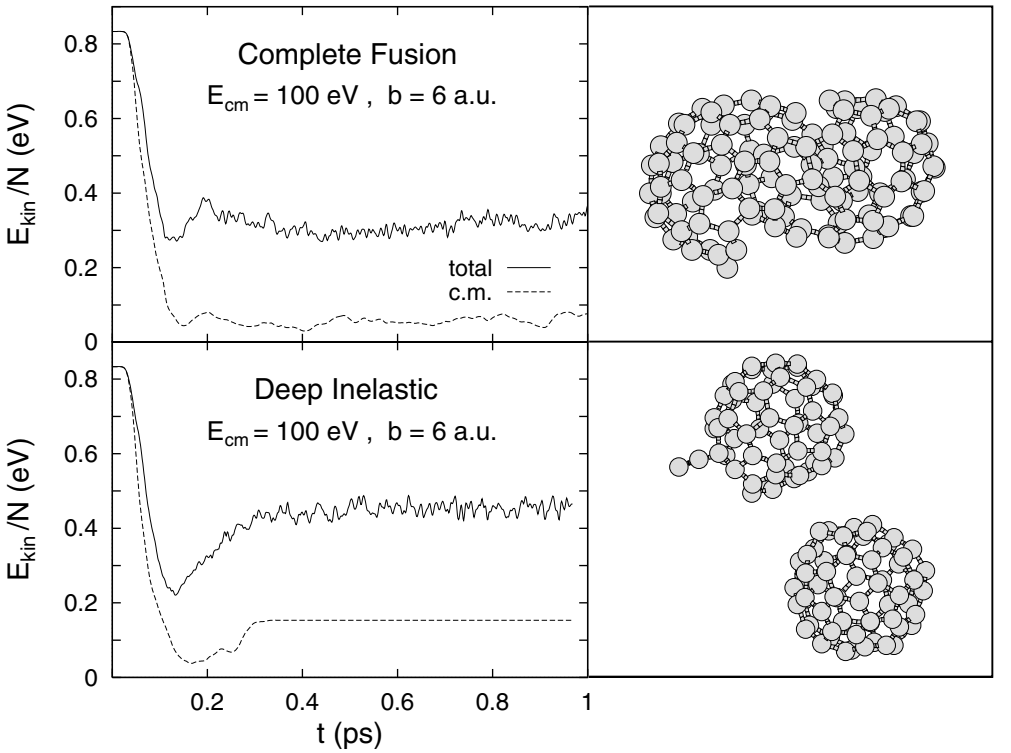

Fig. 1. – Results from QMD simulations of two C_{60}^{+} + C_{60} collisions with the same incident energy and impact parameter (and zero initial temperature). The different random orientations lead to different reaction channels: *complete fusion* and *deep inelastic scattering*. Left: Calculated total kinetic energy per atom (full curves) and center-of-mass kinetic energy per atom of the relative motion between the two colliding fullerenes (dashed curves). Right: Snapshots from the time evolution after the collision.

in table I. Comparing the theoretical values at zero temperature for the three systems, a remarkable increase of the fusion barrier with increasing particle number of the colliding fullerenes can be seen. The relatively large energy thresholds for fullerene fusion (compared to thermal energies) are a consequence of the fast and effective energy transfer from collision energy into internal energy distributed among a lot of vibrational degrees of freedom [5]. Large deformations have to be induced, *i.e.* the closed fullerene structure has to be broken, before a rearrangement of atoms in the overlap region can lead to stable "intercluster" bonds [4].

The theoretical barriers for $T = 0$ are significantly larger than the experimental values (cf. second and fourth columns in table I), which has been understood for C_{60}^{+} + C_{60} to be an effect of the finite cluster temperature in the experiment [5]. The available phase space is considerably enlarged due to the additional energy and the softening of the tight fullerene structure. Unfortunately, the actual cluster temperature in the experiment can be estimated only roughly by indirect methods [15]. We have chosen for our simulations a temperature of $T \approx 2000$ K for projectile and target, which fits into the experimental estimation (1800–2000 K [15]). The resulting fusion barriers for C_{60}^{+} + C_{60}, C_{70}^{+} + C_{60} and C_{70}^{+} + C_{70} agree perfectly with the experimental values (cf. third and fourth columns in table I).

TABLE I. – *Fusion barriers for* $C_{60}^+ + C_{60}$, $C_{70}^+ + C_{60}$ *and* $C_{70}^+ + C_{70}$ *collisions obtained from QMD simulations* [4] *at zero temperature* (*second column*) *and at* $T = 2000$ K *for projectile and target* (*third column*) *compared with the experimental data* (*fourth column, taken from ref.* [15]).

	QMD		Experiment
	$V_B(T=0)$/eV	V_B(2000 K)/eV	V_B/(eV)
$C_{60}^+ + C_{60}$	80	60	60 ± 1
$C_{70}^+ + C_{60}$	94	70	70 ± 6.5
$C_{70}^+ + C_{70}$	104	75	76 ± 4

3. – Mechanism of collision-induced dissociation

In this section we present theoretical studies of the $Na_2^+ + He$ (E_{cm}=80 eV) collision system based on the NA-QMD [12]. The dissociation mechanism of sodium dimers (and of larger clusters Na_N^+, $N = 3, \ldots, 8$) has been investigated recently in full-kinematic correlation experiments by Barat *et al.* [16, 17]. The comparison of the calculated results with that of these experiments represents a first sensitive test of the NA-QMD theory. On the other hand, an NA-QMD analysis allows to obtain a detailed microscopic insight into the excitation and dissociation mechanisms by considering also non-measurable quantities like time and impact parameter dependences of the collision process [18].

Two qualitatively different collision scenarios can been considered depending whether the helium atom interacts primarily with the atomic cores or with the (valence) electrons of the cluster: In the first type of interaction, hereinafter denoted as the *impulse mechanism*, the target atom transfers momentum to one or more atomic cores of the cluster resulting in vibrational excitation and subsequent fragmentation. The *electronic mechanism*, on the other hand, involves excitation of the cluster into a dissociative electronic state leading to the fragmentation owing to electron-vibrational coupling. These two mechanisms are invoked in many other processes too. They are nothing else than the nuclear and electronic components of the "stopping power" of atomic particles inside the bulk.

Important aspects of the fragmentation mechanism are revealed by the correlation between the centre-of-mass scattering angle χ and the relative kinetic energy of the fragments E_{rel}. In fig. 2 the measured as well as the calculated intensities of fragmentation events are shown as a function of χ and E_{rel}. The three maxima observed in the experimental diagram (left part) are nicely reproduced by the NA-QMD calculation (right part). They can be assigned to different dissociation mechanisms: the stretched peak at $\chi \sim 15°$–$30°$ indicates fragmentation via the impulse mechanism because χ increases with increasing relative energy E_{rel}, whereas the peaks at $\chi < 10°$ can be interpreted as electronic fragmentation. They are less dependent on the scattering angle χ and break up into two structures which signals that the atomic fragmentation dynamics is quantized according to the electronic states. In such cases, in principle, a full quantum-mechanical treatment of the whole system is required. In the present case, however, one may relatively easily incorporate quantum effects of the relative motion by projecting the time-dependent wavefunction onto the eigenfunctions and calculating occupation probabilities.

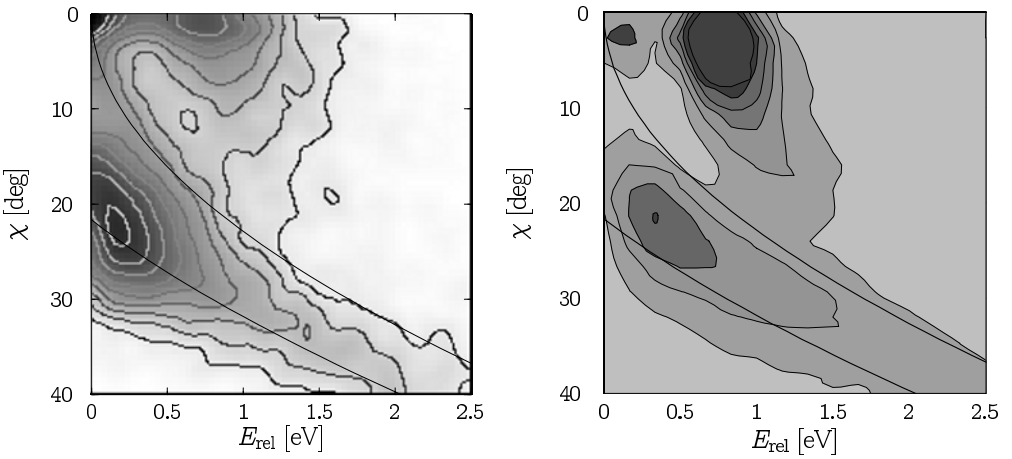

Fig. 2. – Measured (*left part*) and calculated (*right part*) distribution of fragmentation events as a function of the relative energy of the fragments E_{rel} and the centre-of-mass scattering angle χ for collisions $Na_2^+ + He$ (E_{cm}=80 eV). Experimental data are taken from [16]; the curves correspond to an analytical kinematic model [18].

With these probabilities one can randomly choose an eigenstate which determines the fragmentation dynamics henceforth [18].

To gain further insight into the dynamics, the fragmentation probability P_{frag} has been considered as a function of the impact parameter b. Figure 3 shows the impact parameter dependence of $b \cdot P_{\mathrm{frag}}$. Results of NA-QMD calculations are compared with those obtained by QMD calculations where fragmentation can occur only via the impulse (adiabatic) mechanism. The maximum of the adiabatic P_{frag} appears at $b \approx 3a_0$ which is just the half of the atomic distance in Na_2^+ of about $6a_0$. Surprisingly, electronic transitions

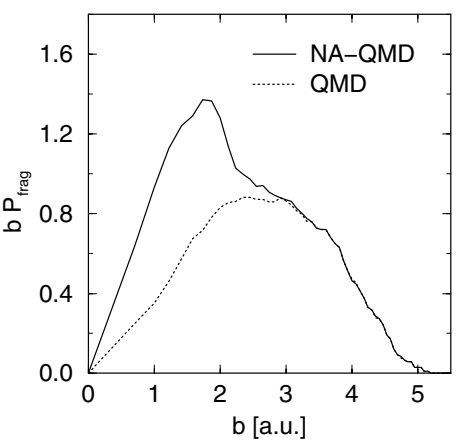

Fig. 3. – Calculated fragmentation probability P_{frag} multiplied by the impact parameter b as a function of the impact parameter for collisions $Na_2^+ + He$ (E_{cm}=80 eV). Adiabatic (*dotted curve*) and non-adiabatic (*solid*) QMD calculations are compared. Note that differences between both calculations are restricted to small impact parameters $b < 3\,a_0$.

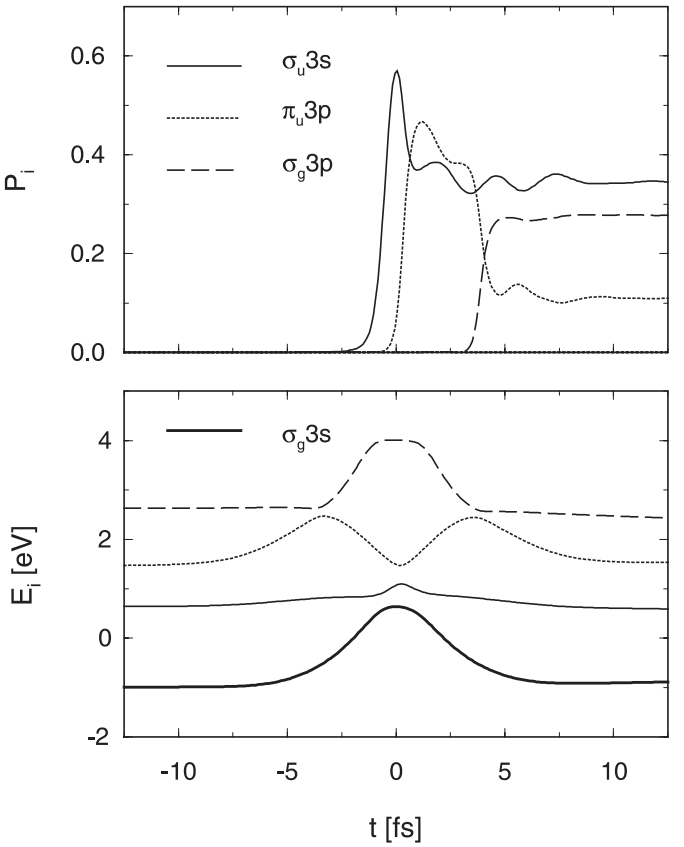

Fig. 4. – Calculated time evolution of the energy levels E_i (*bottom*) and the occupation probabilities P_i (*top*) of the participating orbitals ($i = \sigma_u\, 3s, \sigma_g\, 3p, \pi_u\, 3p$) for a typical collision $Na_2^+ + He$ (E_{cm}=80 eV, b=0). Note that electronic transitions correspond to avoided crossings and appear as a multi-step process.

increase remarkably the fragmentation probability for central collisions only. Therefore, electronic excitations leading to dissociation must be connected with some momentum transfer associated with a small or even vanishing deflection angle. Consequently, only very specific orientations of the dimer with respect to the beam axis can contribute to the electronic dissociation mechanism [18].

One of the questions of interest concerns the relative contribution of the individual electronic states and the time dependence of the electronic transitions. We will focus here on the latter one and show in fig. 4 the occupation probability $P_i(t)$ and the energy levels $E_i(t)$ for the contributing states obtained from a typical central collision. The energy of the initially occupied ground state $E_{\sigma_g 3s}(t)$ is shown too. The various transitions can directly be assigned to the couplings (avoided crossings) between the states during the collision (compare upper and lower parts of fig. 4). Direct transitions from the ground state are observed into the $\sigma_u 3s$ and $\pi_u 3p$ levels, whereas the excitation of $\sigma_g 3p$ happens indirectly via $\pi_u 3p$. Obviously, this multi-step process requires a non-perturbative treatment of the electronic dynamics.

4. – Outlook

One of the most interesting questions concerning the mechanism of cluster-cluster collisions is the existence of collective (flow) effects in multi-fragmentation reactions [6]. Such effects have been predicted [19] and experimentally found [20] in nuclear heavy-ion collisions. Their simultaneous investigation in different fields of physics may reveal some universal features. Corresponding experiments for clusters are in progress [21].

Concerning the non-adiabatic dynamics of clusters the NA-QMD theory offers a broad perspective for future applications: the investigation of charge transfer in cluster collisions, the study of the "stopping power" in finite systems, the analysis of fragmentation in high-energy cluster collisions or the explicit time-dependent treatment of laser excitation and subsequent relaxation of clusters. Investigations of this kind are in progress.

* * *

This work was supported by the DFG through the Schwerpunkt "Zeitabhängige Phänomene und Methoden in Quantensystemen der Physik und Chemie" and by the EU through the HCM networks "Formation, stability and photophysics of fullerenes" and "Collision Induced Cluster Dynamics".

REFERENCES

[1] SCHMIDT R., LUTZ H. O. and DREIZLER R. M. (Editors), *Nuclear Physics Concepts in the Study of Atomic Cluster Physics, Lect. Notes Phys.*, **404** (Springer, Berlin) 1992.
[2] For a review of metallic systems, see SCHMIDT R. and LUTZ H. O., *Comm. At. Mol. Phys.*, **31** (1995) 461; for a review of fullerene collisions see KNOSPE O. and SCHMIDT R., in *Theory of Atomic and Molecular Clusters*, edited by J. JELLINEK (Springer Series on Mesoscopic Phenomena) 1998.
[3] SCHMIDT R., SEIFERT G. and LUTZ H. O., *Phys. Lett. A*, **158** (1991) 231; SEIFERT G., SCHMIDT R. and LUTZ H. O., *Phys. Lett. A*, **158** (1991) 237; KNOSPE O.,SCHMIDT R., ENGEL E., SCHMITT U. R., DREIZLER R. M. and LUTZ H. O., *Phys. Lett. A*, **183** (1993) 332; SCHMIDT R. and LUTZ H. O., *Phys. Lett. A*, **183** (1993) 338.
[4] KNOSPE O., GLOTOV A. V., SEIFERT G. and SCHMIDT R., *J. Phys. B*, **29** (1996) 5163.
[5] ROHMUND F., CAMPBELL E. E. B., KNOSPE O., SEIFERT G. and SCHMIDT R., *Phys. Rev. Lett.*, **76** (1996) 3289.
[6] SCHMIDT R., SCHULTE J., KNOSPE O. and SEIFERT G., *Phys. Lett. A*, **194** (1994) 101; SCHULTE J., KNOSPE O., SEIFERT G. and SCHMIDT R., *Phys. Lett. A*, **198** (1995) 51.
[7] CAR R. and PARRINELLO M., *Phys. Rev. Lett.*, **55** (1985) 2471.
[8] BARNETT R. N., LANDMAN U., NITZAN A. and RAJAGOPAL G., *J. Chem. Phys.*, **94** (1991) 608.
[9] SEIFERT G. and SCHMIDT R., *New J. Chem.*, **16** (1992) 1145.
[10] JELLINEK J., BONAČIĆ-KOUTECKÝ V., FANTUCCI P. and WIECHERT M., *J. Chem. Phys.*, **101** (1994) 10092.
[11] TOMÁNEK D. and SCHLÜTER M. A., *Phys. Rev. B*, **36** (1987) 1208; KIM S. G. and TOMÁNEK D., *Phys. Rev. Lett.*, **72** (1994) 2418.
[12] SAALMANN U. and SCHMIDT R., *Z. Phys. D*, **38** (1996) 153.
[13] RUNGE E. and GROSS E. K. U., *Phys. Rev. Lett.*, **52** (1984) 997.
[14] GROSS E. K., DOBSON J. F. and PETERSILKA M., *Top. Curr. Chem.*, **181** (1996) 81.
[15] ROHMUND F., GLOTOV A. V., HANSEN K. and CAMPBELL E. E. B., *J. Phys. B*, **29** (1996) 5143.
[16] BRENOT J. C., DUNET H., FAYETON J. A., BARAT M. and WINTER M., *Phys. Rev. Lett.*, **77** (1996) 1246.

[17] BARAT M., BRENOT J. C., DUNET H. and FAYETON J. A., *Z. Phys. D*, **40** (1997) 323.
[18] FAYETON J. A., BARAT M., BRENOT J. C., DUNET H., PICARD Y., SAALMANN U. and SCHMIDT R., *Phys. Rev. A*, **57** (1998) 1058.
[19] SCHEID W., MÜLLER H. and GREINER W. , *Phys. Rev. Lett.*, **32** (1974) 741.
[20] For a review see, *e.g.*, STÖCKER H. and GREINER W., *Phys. Rep.*, **137** (1986) 277.
[21] HVELPLUND P., private communication.